CFD validation studies for a high-speed foil-assisted semi-planing catamaran

10 AUTHORS, INCLUDING:

Manivannan Kandasamy
Flow Inc.
36 PUBLICATIONS **175** CITATIONS

SEE PROFILE

Philip Osborne
Golder Associates
59 PUBLICATIONS **677** CITATIONS

SEE PROFILE

Neil J Macdonald
Coldwater Consulting Ltd.
21 PUBLICATIONS **56** CITATIONS

SEE PROFILE

Nic de Waal
Teknicraft
4 PUBLICATIONS **18** CITATIONS

SEE PROFILE

CFD VALIDATION STUDIES FOR A HIGH-SPEED FOIL-ASSISTED SEMI-PLANING CATAMARAN

Manivannan Kandasamy[1], Seng Keat Ooi[1], Pablo Carrica[1], Frederick Stern[1], Emilio F. Campana[2], Daniele Peri[2], Philip Osborne[3], Jessica Cote[3], Neil Macdonald[4], Nic de Waal[5]

[1] IIHR-Hydroscience & Engineering, the University of Iowa
[2] INSEAN- Italian Ship Model Basin, Via di Vallerano 139, 00128 Roma, Italy
[3] Golder Associates, Inc,
[4] Coldwater Consulting Ltd.
[5] Teknicraft Design Ltd

ABSTRACT

This paper details the CFD validation studies carried out as a pre-requisite for multi-fidelity CFD-based design optimization of high-speed passenger-only ferries aimed at reducing far-field wake energy that causes beach erosion. A potential flow code (WARP) and a URANS code (CFDShip) were validated using full-scale measurements of resistance, sinkage, trim, and far-field wake train obtained over a wide range of *Fr* for two high-speed semi-planing foil-assisted catamarans: *Spirit* (LOA-22 m) and 1060 (LOA-17 m). This endeavor posed a unique combination of challenges for CFD modeling: the foil appended geometry required complicated surface overset grids, the effect of the water-jet and wind resistance had to be modeled, and a method had to be devised to extrapolate the calculated near-field elevation to get the far-field wake train using Havelock sources. A more concentrated effort was applied to the URANS verification and validation which forms the focus of this paper. The results show that URANS is able to accurately predict the resistance and motions for both vessels when coupled with models that account for the propulsors and air resistance. The overall accuracy of URANS for the performance analysis of the foil-assisted, semi-planing catamarans was adequate to warrant its use as a tool for subsequent design and optimization of a new vessel with significantly reduced wakes.

1. INTRODUCTION

The Seattle-Bremerton Passenger Only Fast Ferry (POFF) Study was designed to investigate the feasibility of adding POFF service between Seattle and Bremerton. A limiting factor in the development of this link in the past has been the potential for wake-induced erosion of the shoreline in the environmentally sensitive Rich Passage, just east of Bremerton. As part of the study, a new high-speed, semi-planing, foil-assisted catamaran (FAC) vessel that is optimized for wake and total resistance is being designed, developed and will be tested in-situ for determination of impacts. The design and optimization of the new high-speed vessel required computational fluid dynamics (CFD) tools that could predict resistance, motions, and farfield wake. The CFD tools were validated using field data containing powering data, ship motion and far-field wakes of two pre-existing high-speed low-wake FAC vessels, *Spirit* and 1060.

The requirements of accurate ship motion, powering predictions, and far-field wake predictions creates the need for CFD tools that can solve the near-field viscous hydrodynamic forces and capture the far-field wake at a transverse distance of 300 m from the sailing line. Although tremendous advances have been made in the past few years in the development and validation of CFD for ship hydrodynamics (Gorski 2002, Stern *et al.*, 2006), most of these advances have focused on model-scale data (Miller *et al.*, 2006, Carrica *et al.*, 2006) due to the issues involved in collecting full-scale data (Verkuyl and Raven, 2003). Full-scale CFD simulations also have been limited by numerical methods and turbulence modeling. A detailed

discussion of these issues and use of wall functions for full-scale simulations can be found in Bhushan *et al*. (2009). Viscous hydrodynamic CFD has also been restricted to near-field wake studies due to the computational costs of large dense grids required to compute far-field wake data. Heimann *et al*. (2008) and Scragg (2003) have shown that is possible to extrapolate the local free-wave spectrum generated by CFD codes to the far-field by fitting the predicted wave elevations using Havelock sources to a data set by using a minimal number of sources. The waterjet has a significant effect on the trim, and the trim has an effect on both the resistance and the farfield wakes. Kandasamy *et al*. (2009) have shown that the effects of the waterjet on the trim can be modeled using a CFD waterjet model without computationally expensive detailed calculations of the flow through the waterjet.

   The present paper details the work carried out to validate the CFD tools that were applied to the design and optimization of a low wake FAC design. The objectives for the validation process include the accurate prediction of resistance, sinkage, trim and the far-field wave elevations. Details of the EFD data collection methods are briefly presented along with the uncertainty analysis of the data. Further details on the EFD measurements can be found in Osborne *et al*., (2007). For the CFD portion two codes were evaluated for their accuracy in predicting resistance and motions. The first code was the general purpose unsteady Reynolds Averaged Navier-Stokes (URANS)/Detached Eddy Simulation (DES) solver CFDShip-Iowa version 4 (Carrica *et al*, 2007). Computations using the URANS code were carried out at model-scale and the results extrapolated to full-scale. The effect of the waterjet on trim was modeled using the CFD waterjet model (Kandasamy *et al*., 2009). Air resistance was evaluated by simple force calculations based on the frontal area and drag coefficient of the vessels. Calculation of the far-field wake using URANS would require an unfeasibly large domain; so a Havelock code with a source distribution matching the URANS calculated near field wave elevation was used to propagate the wakes to the fair-field. Since no near-field wave elevation data is available, the URANS predictions of the near-field wave elevation and the Havelock source based farfield extrapolation of the near-field data are validated jointly using the farfield wake data. The second code was WARP, a potential flow solver from INSEAN (Bassanini *et al*., 1994) with non-linear free surface condition, able to deal with lifting surfaces, releasing a linearized wake. An iterative procedure accounting for the true sinkage and trim of the ship is solved together with the non-linear free-surface terms. External forces can be applied, and also an actuator disk has been implemented. The presence of a waterjet is also treated in a body-forces type approach.

2. EXPERIMENTAL DATA COLLECTION METHODS AND OVERVIEW OF DATA

   Full-scale vessel trials were conducted with the FAC vessel *Spirit* in February 2005 to provide wake and performance data across a range of operating speeds both with and without interceptors installed on the vessel transom. Wake and vessel performance measurements were subsequently conducted with the FAC vessel *1060* in February 2006 to provide data for validation of the effects of trim and draft on wake generation performance of the Teknicraft FAC design. The tests with *1060* were also designed to assess the potential benefits of utilizing an adjustable-foil catamaran design for a low-wake passenger ferry (Osborne *et al*., 2007).

   The wake measurements involved deployment of multi-point instrument arrays including up to four wave gauges that measured time series of water surface elevations at a range of distances from the sailing line and for a range of vessel speeds. The wave gauge deployment was designed

to enable measurement of wakes with sufficient temporal resolution to resolve the full spectrum of wave heights, periods, direction, and energy generated by the test vessels operating through a broad range of speeds. The sensor array was deployed perpendicular to the sailing line to permit analysis of the dispersion of the wake as it propagates from the sailing line and to validate the dispersion patterns predicted by wake wash models.

On-board instrumentation was deployed on the test vessels during the trials to measure pertinent details of vessel performance. Instruments including a high accuracy dynamic motion sensor with inertial compensation (+/- 0.05^{o} pitch/roll accuracy and +/-0.05m heave accuracy) and a survey grade Global Positioning System (0.01 m horizontal accuracy and 0.02 m vertical accuracy) were installed on the research vessels and the signals multiplexed with navigation software to record the still water trim, the dynamic motion of the vessel (heave, pitch, roll), as well as the precise vertical and horizontal position of the vessel in time for correlation with wake properties.

The vessel trials conducted with *Spirit* and 1060 included multiple passes of the multi-point instrument arrays across a range of speeds (Froude numbers). Typically, between four and six passes were made for any give speed. Wake time series measured at the instrument arrays are analyzed to determine spectral properties (energy and amplitude versus wave period) of the wakes for correlation with vessel operating parameters (speed, trim, and draft). Measured wake parameters were transformed to a common distance of 300 m from the sailing line using a 1D depth and frequency dependent wave transformation approach for comparison with farfield model predictions from the Havelock code.

3. COMPUTATIONAL METHODS
3.1 Viscous Solver

CFDSHIP-Iowa is a general purpose URANS/DES solver developed at IIHR over the last 15 years for ship hydrodynamics applications. For the current simulations, URANS with the blended $k-\omega/k-\varepsilon$ turbulence model (Menter, 1994) was used. The free surface location is predicted by a single phase level set method. A finite difference second order upwind scheme is used to discretize the convective terms of the momentum equations for URANS and solved using the predictor-corrector method. A pressure-implicit split-operator (PISO) algorithm is used to enforce mass conservation on the collocated grids. The pressure Poisson equation is solved using the PETSc toolkit (Belay *et al*., 2002). All the other systems are solved using an alternating direction implicit (ADI) method. A MPI-based domain decomposition approach is used, where each decomposed block is mapped to one processor. The software SUGGAR (Noack, 2005) runs as a separate process from the flow solver to compute interpolation coefficients for the overset grids and communicates with a motion controller (6DOF) within CFDShip-Iowa at every timestep. The software USURP (Boger and Dreyer, 2006) is used to compute area and forces on the surface overlap regions. Fig. 1shows the simulation domain and the overset grids used; the boundary conditions are tabulated in Table 1. A 5-million-point grid was used for all the calculations, based on a grid verification study done on ship-1060. The calculations used 48 processors, and statistical convergence of forces, i.e. oscillations are within 1% of the mean value, was achieved after ~1000 CPU hours.
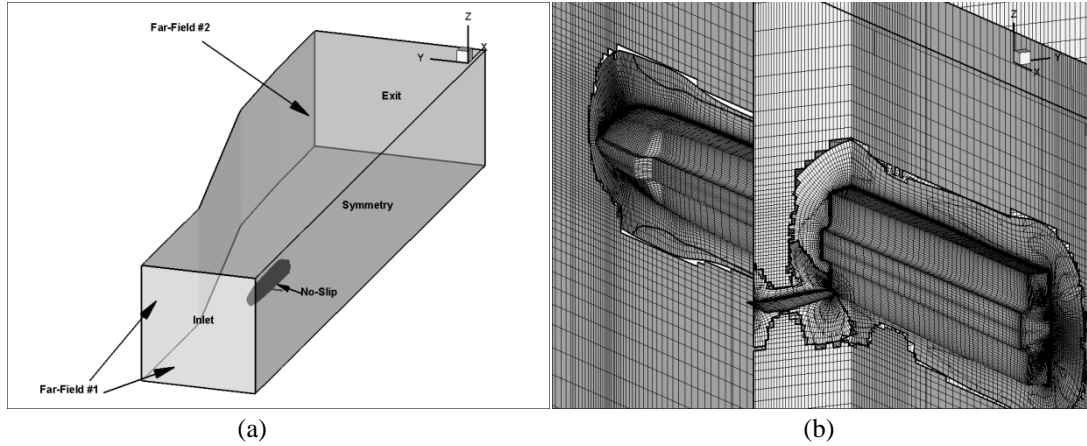
(a)   (b)

Fig. 1. Figures showing a) extent of domain and boundary conditions and b) Overset Grids for simulations that were carried out.

Table 1. Boundary conditions

Description	U	V	W	p
Inlet (x=-0.25)	U=1	V=0	W=0	0
Exit (x=6)	$\dfrac{\partial^2 U}{\partial \mathbf{n}^2} = 0$	$\dfrac{\partial^2 V}{\partial \mathbf{n}^2} = 0$	$\dfrac{\partial^2 W}{\partial \mathbf{n}^2} = 0$	$\dfrac{\partial p}{\partial \mathbf{n}} = 0$
Far-field #1 (y=ymax; z=-1.0)	U=1	$\dfrac{\partial V}{\partial \mathbf{n}} = 0$	$\dfrac{\partial W}{\partial \mathbf{n}} = 0$	0
Far-field #2 (z=0.5)	U=1	V=0	W=0	$\dfrac{\partial p}{\partial \mathbf{n}} = 0$
No-slip (ship-hulls)	0	0	0	-
Symmetry (y=0)	$\dfrac{\partial U}{\partial \mathbf{n}} = 0$	0	$\dfrac{\partial W}{\partial \mathbf{n}} = 0$	$\dfrac{\partial p}{\partial \mathbf{n}} = 0$

The simulations were carried out at model scale with a waterline length of 2 m. This is equivalent to simulating a model scale of 1/9.8 for *Spirit* and 1/7 for 1060. For *Spirit* the resistance, sinkage and trim simulations were carried out at $\mathrm{Fr_L} = U/\sqrt{gL} = 0.61$, 0.91, 1.04 and 1.42, and for 1060 the simulations were carried out at $\mathrm{Fr_L} = 1.32$, 1.49, 1.67 and 1.84, where U is the vessel velocity, g is the gravitational acceleration and L is the waterline length. The model scale friction coefficient (C_{Fm}) from the simulations were extrapolated to full scale C_{Fs} using the ITTC friction line formulae: $C_{Fs} = C_{Fm} (\log Re_m - 2)^2 / (\log Re_s - 2)^2$

3.2 Potential Flow Solver

WARP potential solver (Bassanini *et al*, 1994) is a classical Boundary Element Method (BEM) type solver. Rankine sources together with vortex rings are arranged on the hull geometry and on a portion of the free surface around the ship. Desingularized panels are adopted on the free surface. Derivatives of the velocity potential are obtained analytically. The set of equations are a simple impermeability condition on the body ($\frac{\partial \varphi}{\partial \mathbf{n}} = 0$) and a unified free surface condition:

$$\varphi_{ll} \varphi_l^2 + \frac{\varphi_z}{Fr^2} = 0 . \tag{1}$$

The quadratic term for the velocity potential φ is updated at each iteration, together with the free surface elevation: at the end of an iterative process, the boundary condition is computed on the exact free surface, and the non-linear term is converging to the exact value. Also the wetted portion of the hull is changing according to the computed wave elevation. A different boundary condition is imposed at the transom stern, if present. Simulations are not affected by the scale, since the viscous terms are not directly considered during the solution, and an accurate estimate of the wave resistance is obtained, by pressure integration or by wave cut analysis. Around 3000 panels have been disposed on the hull surface, plus 3000 panels on the free surface. Extension of the considered free surface domain is here quite large, due to the high value of the Froude number, that implies long waves generated by the model: 8 ship lengths astern, 2 ship length fore and 4 ship lengths aside represent the dimension of the fluid domain. The estimated resistance, represented by the wave resistance plus a frictional contribution obtained by means of a locally adapted friction line (based on the local Reynolds number), is applied in reverse along the axis of the waterjet, in order to take into account the effect of the drive force on the sinkage and trim of the hull. The hull position is obtained by the equilibrium of the forces on the hull plus the thrust of the waterjet.

3.3 CFD Waterjet Model

The ITTC Waterjet Performance Prediction Specialist Committee (Van Terwisga, 2005) has developed a model testing procedure for waterjet propulsion by adopting a control volume approach balancing momentum and energy through the waterjet system to arrive at system thrust, thrust deduction, and delivered power. Wilson *et al.* (2005) showed experimentally that the forces and moments created by the operation of a waterjet can affect the pitch and trim of a vessel, which is not dealt with in the ITTC procedures. The need to accurately predict the trim and sinkage in the current study motivated the derivation of an integral force/moment waterjet model for CFD that improved the accuracy of sinkage and trim predictions by providing a set of forces and moments that replicates the effect of the waterjet without requiring detailed modeling of the waterjet (Kandasamy *et al*., 2009). In cases where the detailed flow modeling of the waterjet is not required, the use of a force/moment model becomes attractive. The CFD waterjet model requires limited waterjet geometry (inlet and outlet areas and locations; and weight of working fluid) and several waterjet flow (mass flow rate; inlet pressure force; inlet and outlet momentum correction factors and flow angles; and waterjet induced stern pressure force) input variables. In the current study, since data is unavailable for the waterjet induced inlet/stern

pressure force, the CFD waterjet model couldn't be implemented as desired. Alternatively, the waterjet induced force on the stern for URANS simulations was estimated by conducting simulations with the vessels fixed at the EFD trim but free to heave. These simulations output trim moments from which the stern forces could be calculated.

3.4 Simple Havelock method to extend near-field URANS solution

The distance of the EFD wave gages from the vessel sailing line (y/L > 20) would require a prohibitively large computational domain (x/L > 200, y/L > 20) to capture the wave propagating from the ship. The computational cost for such a large domain resulted in the need for an alternative to the local flow-field solvers to capture the far-field wake.

Heimann *et al.* (2008) have done an intensive review of the different methods that can be used to calculate the far-field wake based on near-field data. The method implemented here is a simplification of the method proposed by Scragg (2003). Scragg (2003) showed that a distribution of Havelock sources could be used to generate far-field waves that matched a measured or computed wave system. Scragg's method required that the input wave data be gathered from a location outside of the local ship wave influence. Time and resource limitations required that the input wave data in the method adopted lie within a region where the local ship wave influence could still be active. In the current method as few Havelock sources and sinks as possible are used to create a wake pattern that will minimize the difference in the near-field wake pattern, specifically the wave length and height at a wake cut along y/L=0.4 predicted by the Havelock source distribution to that obtained from the URANS solution. The authors found that regardless of the Froude number minimizing the errors in wake period and amplitude along a constant line at y/L=0.4 generated the best near-field wake pattern that matched the EFD data. The best combination of Havelock singularities was with one sink along the symmetry plane at the stern, another sink at the stern, and one source at the bow (Fig. 2).
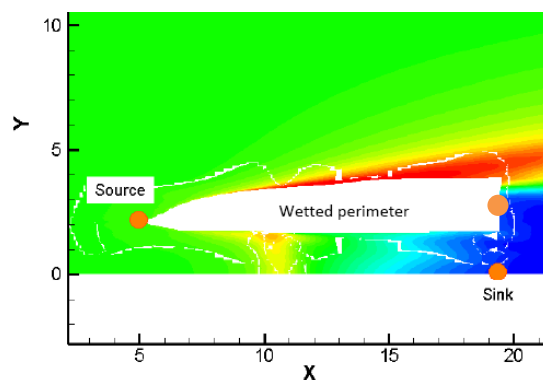

Fig. 2. Example of Source/Sink placement for Havelock source code.

A Havelock source is essentially a steady source traveling underneath the free surface that creates a Kelvin wave pattern. The simplest formulation assumes that the free-surface is linear, infinite water depth and horizontally unbounded. The code used to generate the Havelock sources solves for the polynomial approximations for the Greens function integral as first

proposed by Newman (1987). The Havelock code used in this paper does not account for depth effects.

4 EFD RESULTS AND UNCERTAINTY ASSESSMENT OF EFD FIELD MEASUREMENTS

Weather and tide conditions, variability in vessel operation, as well as slight modifications in vessel load contribute to variability in the vessel and wake data. CFD model results are validated against average vessel trim and sinkage. The average data contain errors associated with variability within any single vessel run as well as for a given Froude number. For 1060, vessel trim varies an average of 12% within runs and up to 26% for a given speed or Froude number; sinkage varies an average of 38% within runs and up to 21% for any given speed or Froude number. The errors are slightly lower for *Spirit* due to its larger size: trim varied 12% within runs and up to 7% for a given Froude number while draft varied as much as 11% for a given Froude number. An example illustrating the variability in vessel wake wash measurements for a given speed is provided in Fig. 3 which shows the variation in the standard deviation of wake height with wake period varying from 2% to 14% of the average wake height. The EFD data presented in the following sections are based on the average of measurements at a given Froude number. In addition, multiple wake events are aggregated for each Froude number to provide the range of measured wake height as well as to establish a trend.
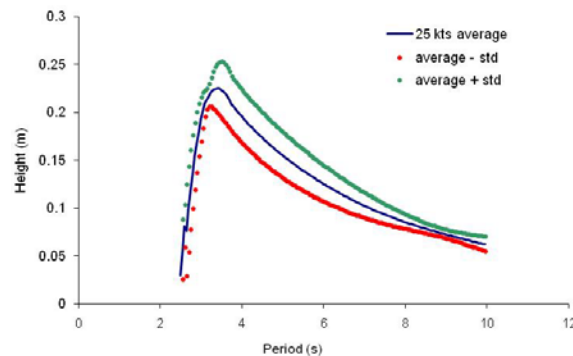

Fig. 3. Variability in vessel wake wash for *Spirit* operating at 25 knots.

5. RESISTANCE, SINKAGE & TRIM

The scaled results for resistance, sinkage and trim for both *Spirit* and 1060 are presented in Fig. 4. EFD resistance values are based on manufacturer powering data and efficiency, provided by Teknicraft. The URANS bare-hull resistance scaled to full-scale for *Spirit* is within 16% of the EFD data and within 23% for 1060 across the Froude number range. For sinkage the errors range from 10.1 to 56.1% for *Spirit* while for 1060 the errors in sinkage range from 4.2 to 28.9%. Although the errors in sinkage values are relatively high compared to other simulations carried out with CFDShip-Iowa it was considered acceptable due to the uncertainty assessment of the EFD data as discussed earlier. Trim errors range from -4.2 to -44.1% for *Spirit* to -31.6% to -164.1% for 1060.

Simulations with the CFD waterjet model improved the prediction of trim with errors reducing to a range of -0.5% to 5.5% for *Spirit* and 3.3% to 56.4% for 1060. The waterjet model does not significantly change the sinkage as compared to the barehull simulation. The predicted resistance are in the same range as that obtained from the barehull simulations with errors ranging from +14.5% to +17.6% for *Spirit* and from +12.2% to 17.4% for 1060.
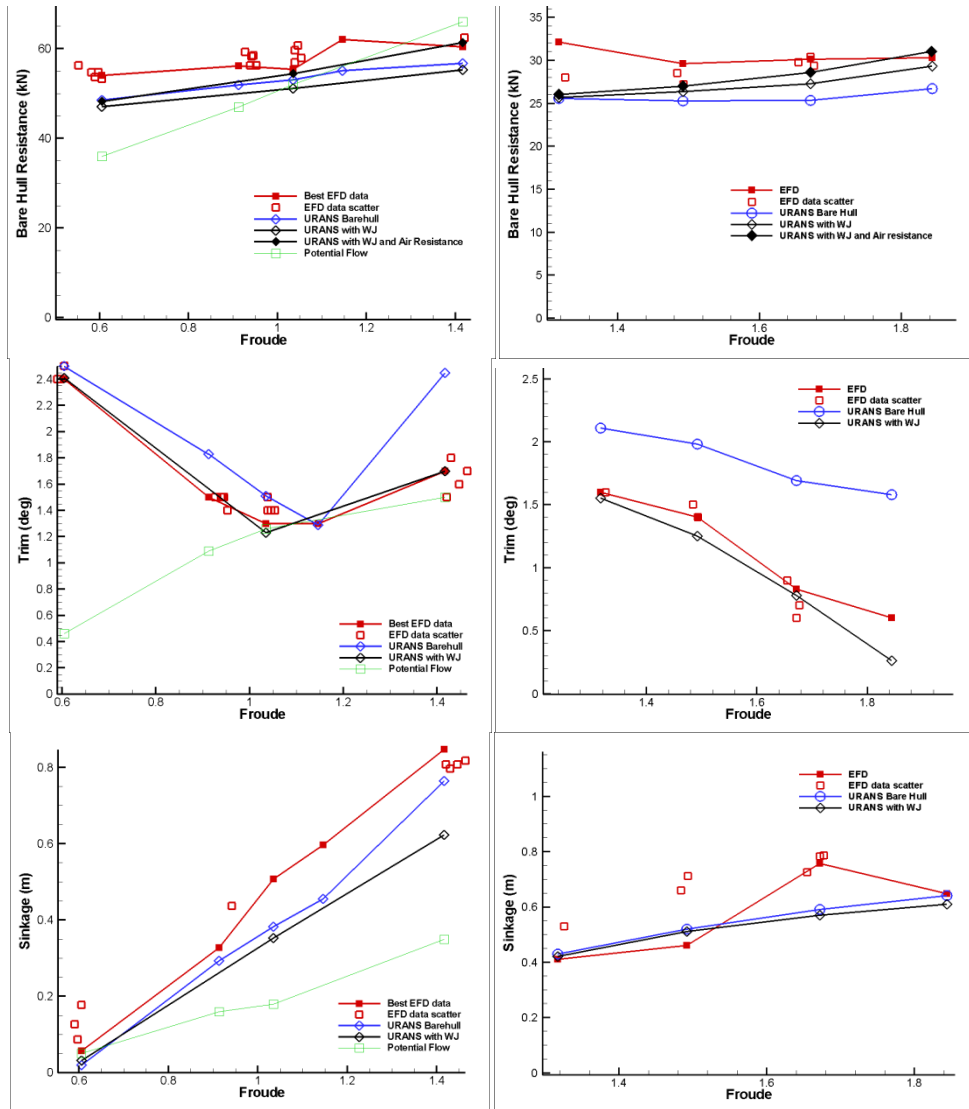

Fig. 4. Resistance, Sinkage & Trim over the Froude number range for *Spirit* and 1060.

The air resistance has not been considered in the simulations as computations were carried out only in the water. The air resistance was then estimated using the frontal areas and drag coefficients supplied by Teknicraft. Adding the values of air resistance to the ship resistance calculated by CFDShip-Iowa reduces the errors for the resistance. Validation of the potential solver WARP with waterjet model has been obtained only for *Spirit* and is included in Fig. 4.

The resistance and trim results match reasonably well (<20%) with the field data for Fr>1. At the lowest Fr (=0.6), the trim is substantially under-predicted.

6. FAR-FIELD WAKE EXTRAPOLATION

Fig. 5 and 6 shows the nearfield match using the Havelock sources for *Spirit* and 1060, respectively, with and without the WJ model.
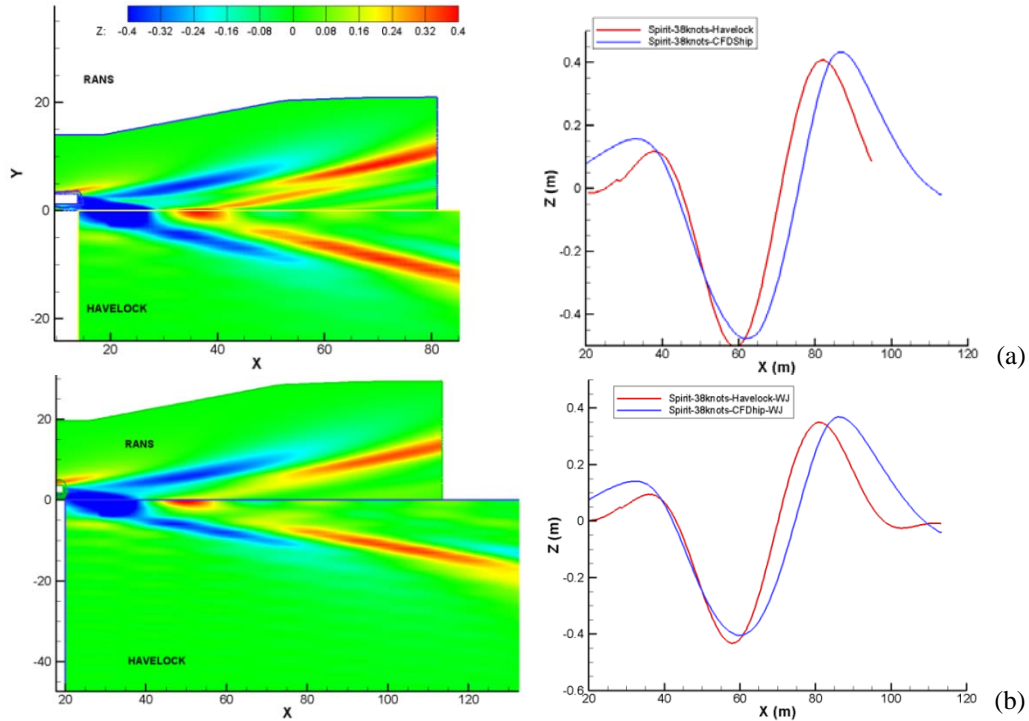

Fig. 5. Near-Field Comparisons for *Spirit* at 38kts (Fr=1.42) :a) Barehull; b) Waterjet.
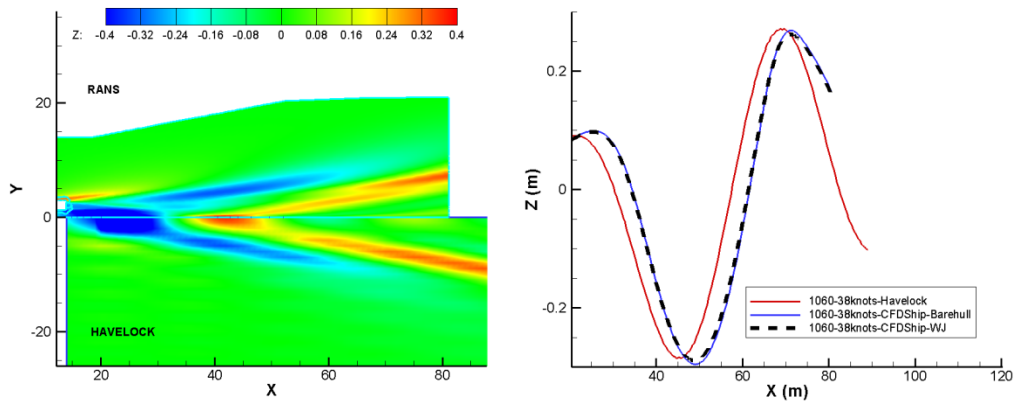

Fig. 6. Near-Field Comparisons for 1060 at 38 kts (Fr=1.67) Barehull and Waterjet

The error for wake height, H, along a cut at y/L =0.4 between the Havelock predictions and URANS ranges from -1.56% to 0.23% for *Spirit* and from -0.16% to 0.89% for 1060. The error for near-field periods, T, between the Havelock predictions and URANS ranges from 8.0% to 14.8% for *Spirit* and from -4.35% to -16% for 1060. The addition of the waterjet reduces the near-field wake height from 0.909m to 0.771m and increases the wake period from 2.5s to 2.6s for *spirit*. However, for 1060 the addition of waterjet does not affect the wake height and period significantly.

Fig. 7 compares the wake-height/period distribution on the wake train obtained by the Havelock source extrapolation of SPIRIT and 1060, with the field data. Fig. 8 compares the wake-energy/period distribution. The calculations using the WJ model are used in the comparisons. The comparisons are made at a distance of 300 m, which is the closest distance of the shore to the sailing line. A general criterion exists, as shown by the line in Fig. 7a, and the farfield wake of the to-be-built POFF should fall under the criterion. The SPIRIT computations show an under-prediction of wake height and energy for periods T < 4s, whereas the 1060 computations show an over-prediction. The sailing lines of both ships were in an average water depth of 30 m. At this depth the depth Froude number is supercritical for velocities of 38 knots and this shallow water effect is not taken into account by the infinite depth Havelock source code.
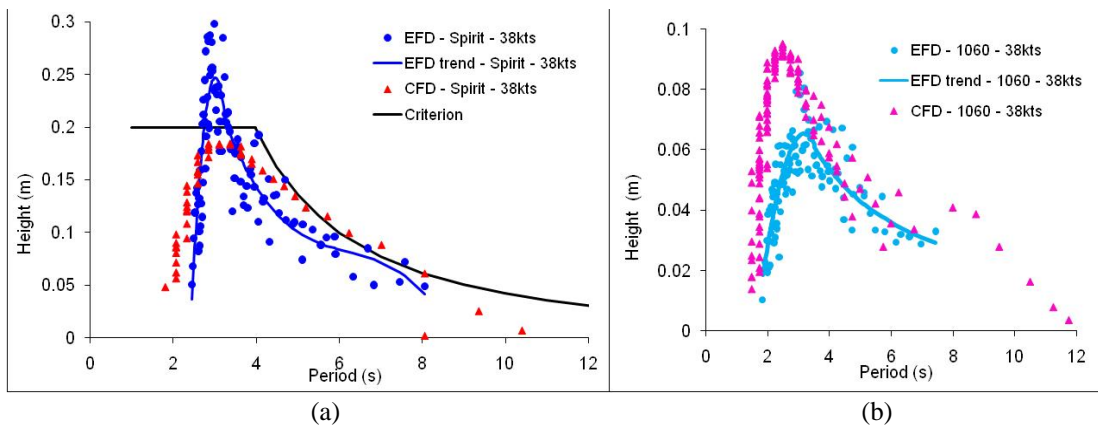

(a)   (b)

Fig. 7. Wake Height vs. Period. (a) Spirit, (b) 1060

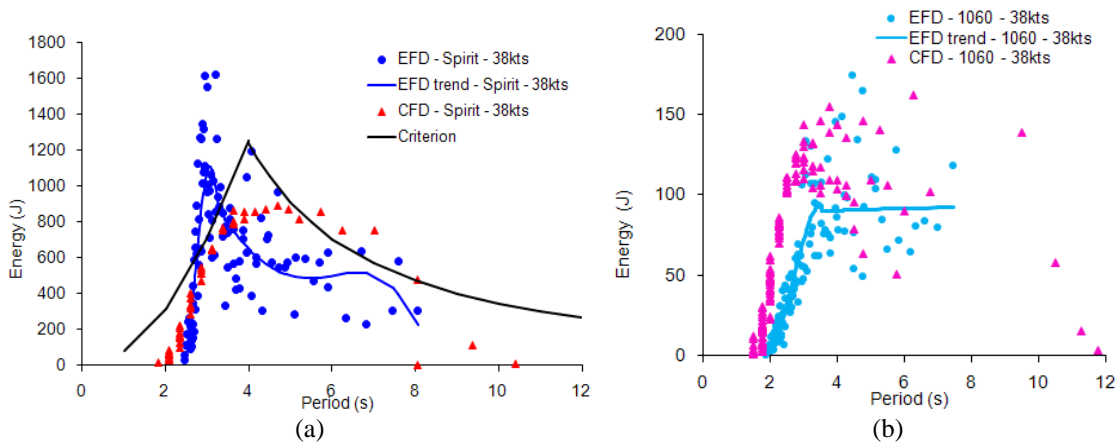(a)   (b)

Fig. 8. Wake Energy vs. Period. (a) Spirit, (b) 1060

7. CONCLUSIONS

The results show that URANS is able to accurately predict the resistance and motions for a full-scale semi-planing catamaran when coupled with models that account for the propulsor and air resistance. Without the propulsor and added air resistance, the errors across the Froude number range for URANS were as follows, for Spirit: 9.6%<E< 15.5% for resistance, 10.1%<E<56.1% for sinkage and -44.1%<E<+0.8% for trim; and for 1060: 19.5%<E<22.6% for resistance, +4.2%<E<28.9%, and -164.1%<E<-31.6% for trim. With the propulsor and added air resistance, the errors in the URANS predictions reduced to the following, for Spirit: 8.6%<E< 12.5% for resistance, 26.4%<E<43.2% for sinkage and -0.5%<E<+5.5% for trim; and for 1060: 2.8%<E<17.5% for resistance, 6.1%<E<31.7%, and 3.3%<E<56.4% for trim. These errors are within the range previously documented for multihull ships using CFDShip-Iowa (Stern *et al.* 2006). The extrapolation of resistance to full scale values using the ITTC friction line is also a contributing factor for the errors. Though the current study motivated the derivation of a CFD water jet model, the model couldn't be implemented as desired due to unavailability of sufficient data and correlations for the waterjet induced stern pressure force. However, the model was implemented using field data measurements of the trim to correct the predicted trim. The potential flow results show good agreement with the data at high Fr, which is the design condition for the new to-be-built POFF. For far-field wake extrapolation, the method developed here which uses a simple infinite depth Havelock source distribution shows good near-field correlation, and reasonable far-field correlation, under-predicting wave height for SPIRIT and over-predicting wave height for 1060. This uncertainty must be taken into account during the design of the new POFF such that a factor of safety is included in the general criterion for wake height. Future work would investigate modifications to the farfield extrapolation method to include shallow water effects by implementing the Scragg (2003) method for finite depth and/or by implementing Boussinesq's equations for ship waves (Jiang *et al.*, 2002) which would include both finite depth and uneven bottom effects. Within the scopes of the present study, the current methods developed during the validation, i.e., extrapolating model scale to full scale using the ITTC friction line, and extrapolating the near-field wave elevation to far-field wake train using Havelock sources, produce satisfactory results to enable their use in the CFD based design of the new low wake POFF (Kandasamy *et al.*, 2009b). The waterjet model could be used as intended for CFD based design in future, if sufficient experimental or detailed simulation data (Kandasamy *et al*, 2009c) is made available to derive correlations for the waterjet induced stern force based on geometry, mass flow rate and inlet velocity ratio.

References

Balay, S., Buschelman, K., Gropp, W., Kaushik, D., Knepley, M., Curfman, L., Smith, B. and Zhang, H. (2002), 'PETSc User Manual'. ANL-95/11-Revision 2.1.5, Argonne National Laboratory.

Bassanini, P., Bulgarelli, U., Campana, E.F., & Lalli, F. (1994). 'The Wave Resistance Problem in a Boundary Integral Formulation'. Surveys on Mathematics for Industry, 4: 151-194

Bhushan, S., Xing, T., Carrica, P.M., & Stern, F. (2009). 'Model- and Full- Scale URANS Simulations of Athena Resistance, Powering and Seakeeping, and 5415 Maneuvering'. submitted to Journal of Ship Research.

Boger, D.A. & Dreyer, J. J. (2006). 'Prediction of Hydrodynamic Forces and Moments for Underwater Vehicles Using Overset Grids'. AIAA paper 2006-1148, 44th AIAA Aerospace Sciences Meeting, Reno, Nevada.

Carrica, P.M., Wilson, R.V., Noack, R.W., & Stern, F. (2007). Ship Motions Using Single-Phase Level Set with Dynamic Overset Grids. Comp. Fluids, 36:1415-1433.

Gorski, J.J., Haussling, H.J., Percival, A. S., Shaughnesssy, J.J., & Buley, G.M. (2002). 'The Use of a RANS Code in the Design and Analysis of a Naval Combatant'. Proceedings of the 24th ONR Symposium on Naval Hydrodynamics, Fukuoka, Japan.

Heimann, J., Hutchison, B.L., & Racine, B.J. (2008). 'Application of the Free-wave Spectrum to Minimize and Control Wake Wash'. Transactions SNAME, 2008

Jiang, T., Henn, R., & Sharma, S. D. (2002). 'Wash Waves Generated by Ships Moving on Fairways of Varying Topography'. Proceeding, 24th symposium on Naval Hydrodynamics, Japan.

Menter, (1994). 'Two-Equation Eddy Viscosity Turbulence Models for Engineering Applications'. AIAA Journal, Vol. 32, No. 8.

Miller, R., Carrica, P., Kandasamy, M., Xing, T., Gorski, J. & Stern, F. (2006). 'Resistance Predictions of High Speed Mono and Multihull Ships with and without Water Jet Propulsors using URANS'. Proceedings of the 26th ONR Symposium on Naval Hydrodynamics ,Rome, Italy, 2006.

Newman, J.N. (1987). 'Evaluation of the wave-resistance Green function - Part 1 - The double integral. Journal of Ship Research'. 31(2):79-90.

Noack R. (2005). 'SUGGAR: a General Capability for Moving Body Overset Grid Assembly'. AIAA paper 2005-5117, 17th AIAA Computational Fluid Dynamics Conference, Toronto, Ontario, Canada.

Kandasamy, M., Ooi, S.K., Carrica, P.M. & Stern, F. (2009a). 'Integral Force/Moment Waterjet Model for CFD Simulations'. Submitted to Journal of Fluids Engineering.

Kandasamy, M., Ooi, S.K., Carrica, P., Stern, F., Campana, E., Peri, D., Osborne, P., Cote, J., Macdonald, N. & Waal, N. (2009b). 'URANS optimization of a high speed foil-assisted semi-planing catamaran for low wake'. 10th International Conference on Fast Sea Transportation, Athens, Greece.

Kandasamy, M., Takai, T., & Stern, F. (2009c). 'Validation of Detailed Waterjet Simulation using URANS for Large High-Speed Sea-Lifts'. 10th International Conference on Fast Sea Transportation, Athens, Greece.

Osborne P.D., Hericks, D.B., & Cote, J.M. (2007). 'Full-Scale Measurements of High Speed Passenger Ferry Performance and Wake Signature'. Proceedings of MTS/IEEE Oceans.

Scragg, C.A. (2003). 'Spectral Representation of Ship-Generated Waves in Finite-Depth Water'. J. of Offshore Mechanics and Arctic Engineering; 125(2): 65-71.

Stern, F., Carrica, P., Kandasamy, M., Gorski, J., O'Dea, J., Hughes, M., Miller, R., Kring, D., Milewski, W., Hoffman, R., & Cary, C. (2006). 'Computational Hydrodynamic Tools for High-Speed Sealift'. Transactions SNAME, 2006; 114.

Van Terwisga, T. (2005). 'Report of the Specialist Committee on Validation of Waterjet Test Procedures'. Proceedings 24th Int. Towing Tank Conference; II:471-508

Verkuyl, J. & Raven, H.C. (2003). 'Joint EFFORT for validation of full-scale viscous flow predictions'. Naval Architect: Jan:41-43.

Wilson, M.B., Gowing, S., Chesnakas, C., & Lin, C-W. (2005). 'Waterjet-hull interactions for sealift ships'. International Conference on Marine Research and Transportation (ICMRT'05), Italy.